International Journal of Research in Engineering, Science and Management
Volume-3, Issue-8, August-2020
journals.resaim.com/ijresm | ISSN (Online): 2581-5792 | RESAIM Publishing

Burn Image Segmentation Based On Mask Regions with Convolutional Neural Network Deep Learning Framework

Prabhakar Kalashetty[1*], Gaurave Sexena[2], Kailesh Patidar[3]
[1]*M.Tech. Student, Department of Computer Science, Sri Satya Sai University of Technology & Medical Sciences, Bhopal, India*
[2,3]*Professor & HoD, Department of Computer Science, Sri Satya Sai University of Technology & Medical Sciences, Bhopal, India*
*Corresponding author: theacadmicpoint@gmail.com

***Abstract*: Burns are life-threatening and particularly terrible and eternal. The effectiveness of a medical decision and, in some instances, the preservation of a patient's life, involves accurate burn portion evaluation and detailed assessment. Present techniques such as straight-ruling, aseptic movie trimming and digital camera photography cannot be repeated and comparable, which result in a major difference in burn injury assessment and impede the establishment of the same assessment criteria. It makes deep learning technology part of a burns treatment that aims to semi-automatically reduce the detection of Burn and to reduce the impact of human error. This essay aims to use the innovative profound education system as a creative solution to the segmentation of burn wounds. We have created a deep-seated iframe ion from the Mask Regions of the R-CNN. This deep learning method is extremely robust in different depths of burn wound and shows outstanding burn wound segmentation. Therefore, only when examining the burn wound, this structure needs an appropriate burn wound image. In hospitals, it is more accessible and more appropriate than conventional methods. It also applies to burnt total body surface (TBSA) quantities.**

***Keywords*: Burning, Effective, Medical.**

1. Introduction

Skin is covered and enveloped in a human body. The clothing is 15 percent of the body weight for the overall weight of a human being. The skin provides feeling, vitamin D production and temperature regulation. The skin gets burned during burning incidents. Some of the main public safety issues is Burn. Humans are severely impaired by fires. The fourth significant cause of accidental fire mortality is Burns.

By fact, the burnt part of the body is killed through the skin and adjacent tissue. During a burning accident, the first care is needed. Specific care is done based on the burned portion size and frequency. The crucial criteria for assessing the extent of burn are component, depth and position of burn. Therefore, the severity of the injuries should be determined by knowing different skin types and the location of the wound. Epidermis and dermis are an essential component of the flesh. The epidermis is considered the thinner surface of the skin, and the thicker inside component is the dermis. The strong connective tissue fibers are used.

Generally, the three different types of burns are superficial dermatic burning, deep dermatic burning and complete burning of spaces. Superficial dermal burns affect the exterior part of the skin or epidermis. Dark, painful and dry is the portion that is impacted. It can also have bubbles. The skin and part of the dermis are affected by deep dermal burns. The blistering and painful part of the burn is rotten. Burns of maximum thickness can damage epidermis and dermis and can be subcutaneous. White or charred the burning portion.

The crucial part of this research is to classify such items to be treated appropriately. Similarly, the images of the skin burn are increased as diagnoses and labelled for the proper treatment. This research aims primarily at establishing a method of classification of images with color loss. The burning of the skin can be subdivided in three categories: superficial dermal fire, extreme skin burning and complete burning width, ion light, intensities of color and shadow from middle to periphery.

Overflowing cures and leaves the scars with proper treatment after i14–10 days; for deep dermal burns and complete brushes in the thickness of the skin, early operations, excision and skin greasing are required, otherwise the cures are slower.

This is important to determine if a burn requires treatment as early as possible. Time-consuming and unreliable treatment raises the danger to the patients. Eventually, multilateral burns are uniform and can be amalgamated over a burning space. To make complicated grafting and cutting brushes, the expert concept is required. Careful analysis under different circumstances guarantees correctly chosen total combustion components.

An automatic device will identify all burns as shown previously. The ion may be classified in the graft foundation. This paper describes the effort to assess the burn depth, particularly the classification of ion grease based on burn and non-grafting. Burning surgeons usually differentiate their

surgical expertise from various burn styles. The accuracy thus ranges from i64 – 76% and i50% between experienced surgeon and beginner.

The modern method uses automated imaging and computers to identify various forms of branding. But, the surgeon will do it when grafting is required.

A. Detection of objects

The most important computer vision issue is study of object identification and subject position. The Convolutionary Network (R-CNN) regions are an object detection method for deep learning in the area of imagery analysis. This system consists of three sections. In the first part selective category-independent regions are created. The second component is a broad neural network derived by a fixed-length feature vector from each field. Collection of linear vector support (SVM) class-specific machines is the last component.

The Quick R-CNN is provided with functional mapping vectors that allow faster training and evaluation. A part of the (RoI) pooling layer is introduced under the R-CNN to prevent duplications of regional proposals. Throughout the classification and regression the author used multi-task failure to accelerate the process. In 2016, the Quicker R-CNN used the RPN to speed up the development of national category-independent proposals. The large deep learning foundation allows the identification of artifacts to reach an acceptable degree.

B. NPR

An extensive search for national concepts is performed in the early object detection system. The organization then suggested a targeted code pressure relief application in i2013 for Uijlings et al. Subsequently, Ren et al. proposed to create high-quality regional proposals across popular characteristic charts. Throughout its development, the RPN used a sliding window on the standard diagram. The RPN then created several ion rectangular frames, and the initial picture is called anchors at each sliding frame. In order to predict target performance and box regression on each key, the RPN network used a tiny neural network. Then the RPN sorted the score of each anchor and took the selfish non-maximum elimination to receive national proposals.

C. Network residual

In i2016, Kaiming et al proposed ResNet. The larger the network is, the more functionality it will have in the convolutionary neural network. While it provides many developments in the picture recognition of the convolutionary neural network, it also poses several different issues. The notorious question of the disappearance / explosion curve, for example, occurs when the network depth deepens. The deep residual learning method will correctly solve the problem of deterioration and gives each layer a connection to the remaining feature. iResNet101 and iResNet50 are the central networks of ResNet.

D. FPN (Pyramid network function)

In 2017, Lin et al suggested FPN. For each dimension, this form of network may construct high level linguistic maps. This comprises three ties bottom-up, top-down and hand. Typically, the FPN's core network is the residual network. At the bottom of each row, the external characteristic map is defined as C2, C3, C4 and C5. The top-down field updates and merges the sampled map to the corresponding bottom-up region with a multiplier of two. The final characteristic chart of 3 to 3 configurations would be applied to every merged index. The actual grades are P2, P3, P4 and P5, respectively. We also introduced the ResNet101 and Atrous FPNs in this report, which we call R101FA.

E. R-CNN mask

Mask R-CNN is an elegant expansion of faster R-CNN, but for successful results it is necessary to construct the mask division properly. R-CNN masks differ in three respects from R-CNN Faster. First, R-CNN masks introduce a branch of the national proposals to estimate the pixel type. The second is that RoI Align is used for syncing pixels between inputs and outputs of the network. Third, the idea of the mask loss. The loss of the mask is only defined for each RoI of a k-th mask associated with ground truth class k.

2. Objectives of the Study

- To test our framework is more convenient and accurate than traditional methods.
- Comparison of feature extraction capability of different backbone networks.
- To propose a new segmentation framework to segment the burn images based on deep learning technology

3. Literature Survey

Mask-Refined R-CNN: A Network for Refining Object Details in Instance Segmentation

The rise of smartphone vision systems and visual sensor networks opens a new age with computer vision features such as target recognition and monitoring. Therefore, the more comprehensive function, like segmentation of instances, will evolve rapidly. Much of the advanced network architectures, such as divisioning, are based on R-CNN mask [1]. However, experimental results confirm that the R-CNN mask does not always successfully forecast instance information.

DeepLab: Extreme convolutionary grid, atrous convolution, and totally connected CRF segmentation.

Within this research, we tackle the job of conceptual image segmentation with Deep Learning and experimentally illustrate three key contributions with substantial functional value. Second, we emphasize the convolution of upsampled filters in complex prediction tasks as an efficient process [2].

A Broad Convolutionary Radiographic Picture System for Gender & Assessment at Bit Plane stage.

Evaluation of a person's age by bones is a crazy manner in

which human talents may be properly calculated. In the past, several efforts have been made to estimate a person's chronological age on the basis of various discriminatory characteristics in wrist X-rays [3]. The permutation and variation of such features include a variety of classes with adequate precision. Gender assessment is conducted with images of left-hand wrist radiographs in this article for persons aged 1-17 years. A fully-automated solution is proposed in the process of radiograph acquisition to remove intermittent noise caused by uniform lighting [4].

Broad research driven stroke management: a clinical practice analysis.

Stroke is a significant source of long-term incapacity and the outcome is immediate. However, not all patients are diagnosed rapidly. There has been significant exposure to the usage of neuroimages for the purpose of assessing possible gains by recognizing parts of ischemia that are yet not cell dead [5]. The infusion/diffusion discrepancy is potentially seen as an early warning tool, but penumphal trends are a flawed predictor of health results.

4. Materials and Methods

In that article we used a new method for using the state-of-the-art deep-learning system Mask R-CNN. We changed the Mask R-CNN to suit our dataset to obtain a more optimized result and a faster training speed. In the backbone network, we changed the loss function of the class branch and embraced Atrous Convolution. We tried several mainstream backbone networks to achieve a better segmentation result and the R101FA showed the best segmentation results.

Set of data: We operated with the Wuhan Hospital No. 3 Burn Department between December 2017 and June 2018. Wuhan Hospital No. 3 and Wuhan University's Tongren Hospital received ethical approvals. The informed consent has already been signed by the patients used in this research.

We used our smartphone to collect images of fresh burn injuries in the hospital every day to get adequate data. Then, in the format Common Objects in Context (COCO), we used our software to annotate burn images and save marked contents. Figure 2 displays the annotated script. We have carefully annotated the burn images under the guidance of professional doctors, thus ensuring the accuracy of this framework, and avoided confusing parts such as gauze and blood stains as wounds. We eventually annotated 1000 burn pictures for training with the help of doctors and nurses and another 150 for assessment.

5. Results

Characterization of burn:

The four main wounds are listed below:

1. Superficial dermal burn,
2. Superficial burns of partial thickness,
3. Seep burns of partial thickness and
4. Burns of complete thickness.

The four depths of burns in four photos are shown below.

(a) (b) (c) (d)

Fig. 1. A–D, Different burn depth. From left to right is superficial, superficial thickness, deep partial thickness, and full-thickness burn

In the past, whole or part segmentation image processing techniques also use evolutionary curvilinear boundaries because of their adaptive ability and templates for internal image structures. In this article, we conclude that the burn has no uniform boundaries. In addition, different wound depths make segmentation more difficult. Traditional technologies no longer work in the burn segment if all burn situations are to be segmented. Therefore, we adopt the profound learning framework for segmentation.

A. Result of segmentation

This paper primarily segments burn wounds without classifying the wound's size. To show the stability and capacity to generalize our work, however, we have selected 150 pictures to evaluate our approach. Such images of various burn part sizes and different burn depth images were combined with the aid of qualified doctors.

B. Various sizes segment

The first advantage is that the different sizes of burn wounds can be segmented by the model. The experiment showed a high strength of the various burn wound sizes in our model. We have chosen the four burn wound depths. As shown in the figure. 8, in the percent of TBSA, our model performed fine segmentation < 5 percent burn wound. In addition, our model has also done very well for the broad burn region.

Fig. 2.

Segmentation consists of the different sizes of burn wounds. The first and second rows show the percentage of TBSA< i5% injuries and the results of iR101FA segmentation. The third and fourth rows display TBSA> 20% wounds and iR101FA (R101FA Residual Network-101 with atrocious pyramid network convolution) results in segmentation.

C. *Various depth segments*

There are many reasons for burning such as high-temperature gas and flame. Hydrothermal fluid. Furthermore, these reasons can lead to various depths of burn wounds. Owing to the heterogeneity of each burn size, the complexity of segmentation increases. However, we can successfully segment the different depths of the burn wound in our model.

Fig. 3. Results of various depths of burned wound. Such four lines are thin, thin, deep partial and dense burning from top to bottom

D. *Comparison of process*

Our methods were contrasted with conventional methods and modern methods.

E. *Classical approaches*

Traditional approaches often use the image's edge characteristics or spectral characteristics to complete image segmentation. We tried our Watershed Algorithm photos in this post. The Watershed algorithm is based on the picture edge and is also seen in the photograph. Much of the time this algorithm uses the color histogram to pick the color to be. Yet the burn wound in the fire images has many colors. It made the identification of burn casualties complicated with the algorithm. It element. Finally, we tried to boost segmentation with a different parameter, we can see that in a complex picture environment the Watershed Algorithm could not show good segmentation.

F. *Modern approaches*

In the recent years, the deep-learning image segmentation approach has achieved outstanding results. Therefore, we selected different architectures as our backbone network. Such networks are IV2RA, R101A, R101FA. They are the backbone networks.

For training, we set 20 epochs for IV2RA and R101A for the best training impact. But we set 16 epochs in our method. 1000 iterations were included in each epoch. First, the loss reduction in the different backbone networks will be seen. As Fig reveals, we can observe that our method can get a better result reduction in losses than the other two backbone networks. And our system used lesser cycles than the compared backbone networks.

Fig. 4.

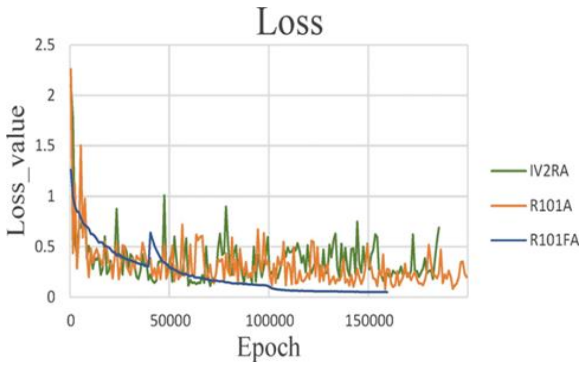

Fig. 5. Epoch vs. Loss value

Loss reports from various backbone networks. IV2RA InceptionV2-residual network of atrocious chaos, R-101A-Residual network-101 of atrocious turmoilization and R-101FA-Residual network-101 of atrocious chaotic.

DC%=1002TPFP+2TP+FNDC%=1002TPFP+2TP+FN(7)

The number of false positives is the FP value in depth. The false positive is the incorrect segmented pixels. The number of false negatives is the FN. The false negative reflects the non-segmented goal pixels. TP is the constructive reality. The true positive is the right pixel segmentation. Therefore, the DC value of the different backbone networks is determined.

Table 1 Average Dice's coefficient (DC) value and prediction speed per picture

From: Burn image segmentation based on Mask Regions with Convolutional Neural Network deep learning framework: more accurate and more convenient

Model name	Average DC value	Prediction speed (per/second)
R101FA (our method)	84.51*	0.374*
IV2RA	83.02	0.538
R101A	82.04	0.519

*The highest average DC value in different models

*The fastest prediction speed in different models

R101FA residual network-101 with atrous convolution in feature pyramid network, *IV2RA* inceptionV2-residual network with atrous convolution, *R101A* residual network-101 with atrous convolution

From the DC values, we find the highest precision in our backbone network R101FA.

To evaluate our model in more detail, we have chosen the various burn images. Total 120 pictures of various types of burn depths have been selected. There were twenty surface burns, 50 superficial burns of thickness, 40 deep burns of part thickness and ten full thickness burns. Due of a lack of burn images we were only able to examine 10 for the full-thickness burn. Next, so we can determine the DC values for the various backbone networks.

Table 2 Dice's coefficient (DC) values of different burn depth in different models

From: Burn image segmentation based on Mask Regions with Convolutional Neural Network deep learning framework: more accurate and more convenient

Burn depths	Model name		
	R101FA (our method)	IV2RA	R101A
Superficial	89.7*	83.61	77.37
Superficial thickness	85.21*	82.52	84.91
Deep partial thickness	84.54*	84.44	81.96
Full-thickness burn	81.12	74.56	83.5*

*The highest average DC value of this burn depth in different models
R101FA residual network-101 with atrous convolution in feature pyramid network, *IV2RA* inceptionV2-residual network with atrous convolution, *R101A* residual network-101 with atrous convolution

As we can see, the segmentation of our model is superficial and deep partial thicknesses was better. Just because of the absence of full density of burn images, our model produced the results for overall density burns slightly worse as compared to the other models.

Similarly, most of the patients had extensive clinical burn. Our method need to show an excellent results in this field. We have selected different images of burn part size to evaluate various models. Results are shown in Table 3.

Table 3 Dice's coefficient (DC) values of different burn sizes in different models

From: Burn image segmentation based on Mask Regions with Convolutional Neural Network deep learning framework: more accurate and more convenient

Burn sizes	Model name		
	R101FA (our method)	IV2RA	R101A
%TBSA < 5%	83.6	86.48	86.63*
5% < %TBSA< 20%	86.13	88.06*	84.85
%TBSA> 20%	81.27*	72.33	74.13

*The highest average DC value of this burn size in different models
R101FA residual network-101 with atrous convolution in feature pyramid network, *IV2RA* inceptionV2-residual network with atrous convolution, *R101A* residual network-101 with atrous convolution

As we can see, the IV2RA is having the highest average DC value of 5% < 20% TBSA and the R101A has the lowest average DC for 5% TbSA wounds < 5%. Similarly, our method is carrying the highest average DC of 20% TBSA wounds and also give very good results in 2 other dimensions.

The prediction time for every picture must be short to ensure successful hospital care. We contrasted the predictive time of the different backbone networks. As shown in Table 1, our models only needed 0.37 s in order to predict a picture that was the fastest prediction.

6. Discussion

Burn image segmentation is the first step in the intelligent treatment of burn wounds. Accurate segmentation is required for follow-up treatment. In this post, we give a technique for separating the pictures. This system increases segmentation accuracy and leads to the brenning clinic relative to the old process. However, certain issues do have to be addressed in this sense. As we know, learning technology needs detailed data to correctly interpret the pattern. This model was equipped with approximately 1000 images due to the difficulty of its data processing and annotation. The bad segmentation reveals some burning pictures on the platform. In fact, our machine cannot determine the extent of the burn bite. The determination of wound extent information will be paired with the medical skill of the practitioner, which ensures that even non-professionals the documentation method is extremely nuanced and confusing. We then collect correct data sets to train the iframe in order to improve segmentation precision. To order to identify the burn wound depth to this context, we can also use the specialist to label details on burn wound depth. And we'll then use the calculation framework for our burn part.

7. Conclusion

The paper has provided us a new segmentation system for the computational segmentation of burn photos focused on deep learning. In the comparison experiment, we compared the function extraction capabilities of the different backbone networks. The R101FA backbone network provides the most accurate and reliable performance. Ultimately, 150 pictures had an overall precision of 84.51%. Our solution in practice is better than conventional approaches, only a suitable RGB injury picture is needed. This provides the facility with enormous advantages. This deep learning method is extremely robust in different depths of burn wound and shows outstanding burn wound segmentation. Therefore, only when examining the burn wound, this structure needs an appropriate burn wound image. In hospitals, it is more accessible and more appropriate than conventional methods. It also applies to burnt total body surface (TBSA) quantities.

References

[1] Gethin G, Cowman S. Wound measurement comparing the use of acetate tracings and Visitrak digital planimetry. J ClinNurs. 2006;15(4):422–7.
[2] Haghpanah S, Bogie K, Wang X, Banks PG, Ho CH. Reliability of electronic versus manual wound measurement techniques. Arch Phys Med Rehabil. 2006;87(10):1396–402.
[3] Rogers LC, Bevilacqua NJ, Armstrong DG, Andros G. Digital planimetry results in more accurate wound measurements: a comparison to standard ruler measurements. J Diabetes Sci Technol. 2010;4(4):799–802.
[4] Sheng WB, Zeng D, Wan Y, Yao L, Tang HT, Xia ZF. Burn Calc assessment study of computer-aided individual three-dimensional burn part calculation. J Transl Med. 2014;12(1):242.
[5] Cheah AKW, Kangkorn T, Tan EH, Loo ML, Chong SJ. The validation study on a three-dimensional burn estimation smart-phone application: accurate, free and fast? Burns Trauma. 2018;6(1):7.